Nucleic Acids Research, 1997, Vol. 25, No. 10 **1935–1942**

# Comparison of the base pairing properties of a series of nitroazole nucleobase analogs in the oligodeoxyribonucleotide sequence 5′-d(CGCXAATTYGCG)-3′

**Donald E. Bergstrom[1,2,*], Peiming Zhang[2] and W. Travis Johnson[1]**

[1]Department of Medicinal Chemistry and Molecular Pharmacology, Purdue University, West Lafayette, IN 47907, USA and [2]Walther Cancer Institute, Indianapolis, IN 46208, USA

Received January 10, 1997; Revised and Accepted March 31, 1997

## ABSTRACT

**The nucleoside analogs 1-(2′-deoxy-β-D-ribofuranosyl)-3-nitropyrrole (9), 1-(2′-deoxy-β-D-ribofuranosyl)-4-nitropyrazole (10), 1-(2′-deoxy-β-D-ribofuranosyl)-4-nitroimidazole (11) and 1-(2′-deoxy-β-D-ribofuranosyl)-5-nitroindole (21) were incorporated into the oligonucleotide 5′-d(CGCXAATTYGCG)-3′ in the fourth position from the 5′-end. Procedures for synthesis of two of the nitroazole nucleosides, 10 and 11, were developed for this study. Each of the nitroazoles was converted into a 3′-phosphoramidite for oligonucleotide synthesis by conventional automated protocols. Four oligonucleotides were synthesized for each modified nucleoside in order to obtain duplexes in which each of the four natural bases was placed opposite (position 9) the nitroazole. In order to assess the role of the nitro group on base stacking interaction, sequences were also synthesized in which the fourth base was 1-(2′-deoxy-β-D-ribofuranosyl)pyrazole. Corresponding sequences containing an abasic site, as well as sequences containing inosine, were synthesized for comparison. Thermal melting studies yielded $T_m$ values and thermodynamic parameters. Each nucleoside analog displayed a unique pattern of base pairing preferences. The least discriminating analog was 3-nitropyrrole, for which $T_m$ values differed by 5°C and $\Delta G_{25°C}$ ranged from –6.1 to –6.5 kcal/mol. 5-Nitroindole gave duplexes with significantly higher thermal stability, with $T_m$ values varying from 35.0 to 46.5°C and $-\Delta G_{25°C}$ ranging from 7.7 to 8.5 kcal/mol. Deoxyinosine (22), a natural analog which has found extensive use as a universal nucleoside, is far less non-discriminating than any of the nitroazole derivatives. $T_m$ values ranged from 35.4°C when paired with G to 62.3°C when paired with C. The significance of the nitro substituent was determined by comparison of the base pairing properties of a simple azole nucleoside, 1-(2′-deoxy-β-D-ribofuranosyl)pyrazole (12). The pyrazole-containing sequences melt at 10–20°C lower than the corresponding nitropyrazole-containing sequences. On average, the pyrazole-containing sequences were equivalent in stability (average $\Delta G$ = –4.8 kcal/mol) to the sequences containing an abasic site (average $\Delta G$ = –4.7 kcal/mol).**

## INTRODUCTION

Recent studies on 3-nitropyrrole deoxyribonucleoside and related analogs suggest that these compounds may have some utility as universal nucleic acid bases. Oligonucleotides containing the deoxyribonucleotides of 3-nitropyrrole (1,2) or 4-, 5- or 6-nitroindole (3,4) have been determined as functioning as primers for dideoxy sequencing and PCR. Melting studies on oligonucleotides containing the deoxyribonucleotides of 3-nitropyrrole (1), 4-, 5- or 6-nitroindole (3) and acyclic analogs of 5-nitroindazole and 4-nitroimidazole (5) have demonstrated that the nitroazoles do indeed show less discrimination in their base pairs with the four natural DNA bases than other types of analogs investigated as universal base candidates.

As part of our investigation to probe the effects of nitroazoles on duplex association we have carried out a study that includes a comparison of the deoxyribonucleosides of 3-nitropyrrole (**9**), 4-nitropyrazole (**10**), 4-nitroimidazole (**11**), pyrazole (**12**), 5-nitroindole (**21**), hypoxanthine (**22**) and an abasic spacer, 1,2-dideoxyribose (**23**) (Fig. 1). This study was designed to allow us to gain additional insight into the significance of electronic structure and heterocyclic size as a guide for the development of more effective universal spacers for duplex nucleic acids.

## MATERIALS AND METHODS

### General procedures

NMR spectra were recorded using a Bruker AC 250 or a Varian VXR-500S spectrometer. $^1$H and $^{13}$C signals were internally referenced to TMS, while 85% phosphoric acid was utilized as an external standard for all $^{31}$P spectra. FAB and MALDI mass spectra were recorded by the mass spectroscopy laboratories of the

*To whom correspondence should be addressed at: Department of Medicinal Chemistry and Molecular Pharmacology, Purdue University, West Lafayette, IN 47907, USA. Tel: +1 317 494 6275; Fax: +1 317 494 9193; Email: bergstrom@pharmacy.purdue.edu

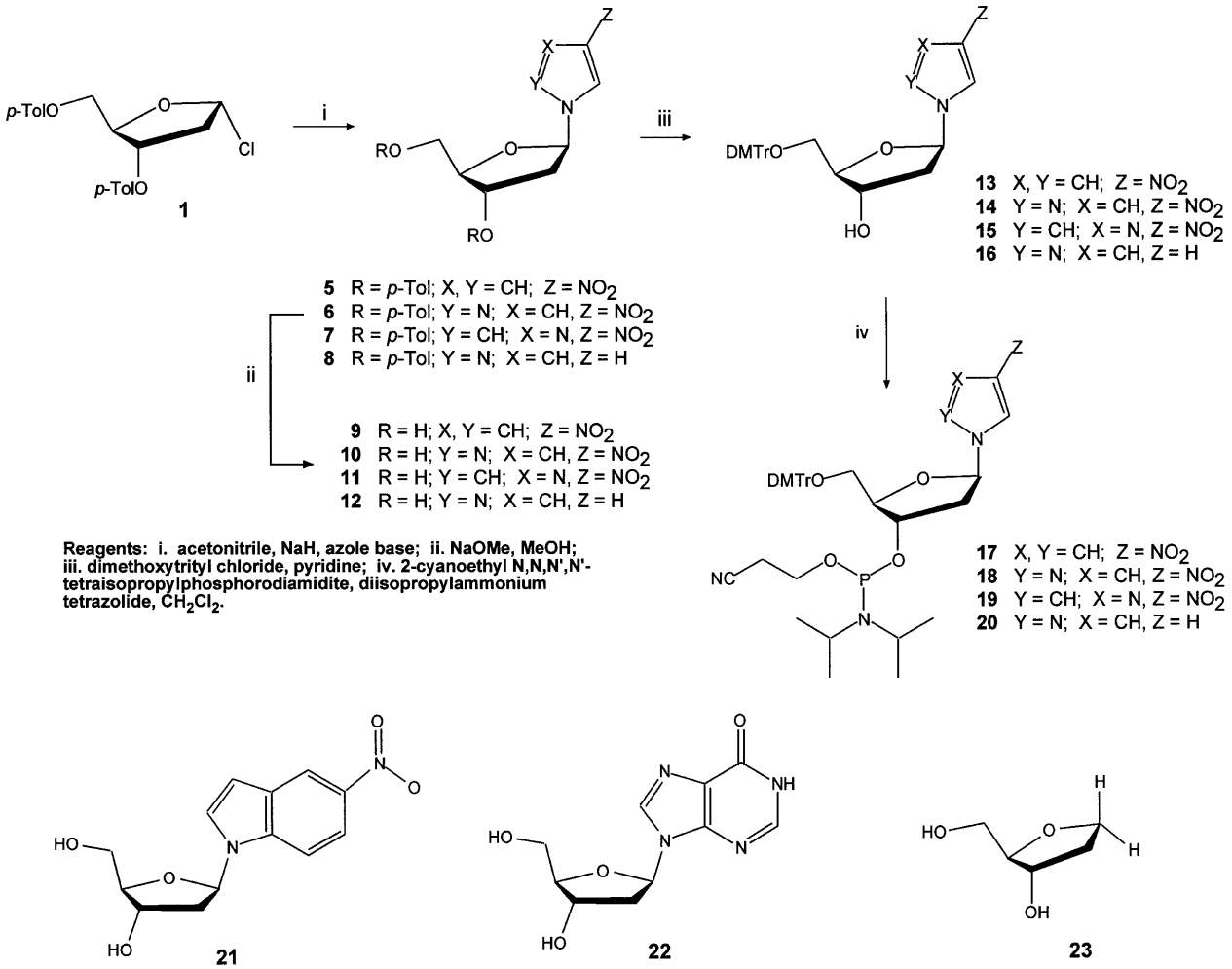


**Figure 1.** Deoxyribonucleoside analogs: 1-(2′-deoxy-β-D-ribofuranosyl)-3-nitropyrrole (**9**), 1-(2′-deoxy-β-D-ribofuranosyl)-4-nitropyrazole (**10**), 1-(2′-deoxy-β-D-ribofuranosyl)-4-nitroimidazole (**11**), 1-(2′-deoxy-β-D-ribofuranosyl) pyrazole (**12**), 1-(2′-deoxy-β-D-ribofuranosyl)-5-nitroindole (**21**), deoxyinosine (**22**) and 1,2-dideoxyribose (**23**) and synthesis of 1-(2′-deoxy-5′-*O*-dimethoxytrityl-β-D-ribofuranosyl)azole 3′-*O*-(2-cyanoethyl-*N*,*N*-diisopropyl)phosphoramidites.

Department of Medicinal Chemistry and Molecular Pharmacology or Department of Biochemistry, Purdue University. Elemental analysis was performed by the Microanalysis Laboratory, Department of Chemistry, Purdue University. Analytical thin layer chromatography (TLC) was carried out on pre-coated Whatman 60 F254 plates. Chromatotron preparative chromatography plates were prepared using silica gel 60 PF254 containing a gypsum binding agent manufactured by Merck. Anhydrous solvents were freshly distilled from the appropriate drying agents or purchased from Aldrich Chemical; all other chemicals were of reagent grade or better quality and used as received.

## Synthetic procedures

*1-(2′-Deoxy-3,5-di-O-p-toluoyl-β-D-ribofuranosyl)-4-nitropyrazole (6).* To a solution of 4-nitropyrazole (**3**) (6) (0.25 g, 2.2 mmol) in anhydrous acetonitrile (10 ml) was added 95% NaH (0.048 g, 1.9 mmol) under a nitrogen atmosphere. The mixture was stirred for 15 min and then 2-deoxy-3,5-di-*O*-*p*-toluoyl-α-D-erythro-pentosyl chloride (**1**) (7) (0.75 g, 2.0 mmol) added. After 1 h, the crude reaction mixture was filtered, the insoluble salts washed with acetonitrile and then the filtrate was evaporated under reduced pressure to an oily residue. The crude product was purified by chromatography on a chromatotron plate (4 mm, silica gel) eluting with hexane/acetone. The final UV absorbing fractions were combined, evaporated under reduced pressure and dried *in vacuo* to give **6** (0.76 g, 75%) as a white solid: $R_f$ = 0.34 (hexane/acetone 3:1); m.p. 137°C; MS-FAB *m/z* 353.0 ($C_{21}H_{21}O_5^+$), 466.0 ($MH^+$); high resolution MS-FAB *m/z* $MH^+$ (calculated 466.1614, found 466.1609); $^1$H NMR 500 MHz (acetone-$d_6$) δ 8.85 (s, H-5, 1 H), 8.23 (s, H-3, 1 H), 7.98–7.91 (m, p-Tol, 4 H), 7.37–7.30 (m, p-Tol, 4 H), 6.48 (triplet, H-1′, *J* = 6.0 Hz, 1 H), 5.92–5.89 (m, H-3′, 1 H), 4.71–4.54 (m, H-4′, H-5′, H-5″, 3 H), 3.27–2.87 (m, H-2′, H-2″, 2 H), 2.43 (s, CH3 p-Tol, 3 H), 2.40 (s, CH3 p-Tol, 3 H). Analysis: calculated for $C_{24}H_{23}N_3O_7$: C, 61.92; H, 4.98; N, 9.03; found: C, 61.54; H, 4.88; N, 9.09.

*1-(2′-Deoxy-β-D-ribofuranosyl)-4-nitropyrazole (10).* To a solution of 1-(2′-deoxy-3,5-di-*O*-*p*-toluoyl-β-D-ribofuranosyl)-4-nitropyrazole (**6**) (0.75 g, 1.6 mmol) in anhydrous methanol (160 ml) was slowly added a 0.2 M solution of sodium methoxide (24 ml). The solution was stirred overnight, cooled to 0°C and then neutralized to pH 7 by the slow addition of glacial acetic acid. The neutral solution was evaporated under reduced pressure to an oil. The

residue was dissolved in methanol and separated by chromatography on silica gel ($CHCl_3$/methanol 3:1). The final fractions were combined, evaporated under reduced pressure and dried *in vacuo* to give 1-(2′-deoxy-β-D-ribofuranosyl)-4-nitropyrazole (**10**) (206 mg, 56%) as a white foam. $R_f$ = 0.30 ($CHCl_3$/methanol 9:1): high resolution MS-FAB *m/z* $MH^+$ (calculated 230.0777, found 230.0769); $^1$H NMR 500 MHz (methanol-$d_4$) δ 8.81 (s, H-5, 1 H), 8.15 (s, H-3, 1 H), 6.15 (triplet, H-1′, *J* = 5.9 Hz, 1 H), 4.52–4.59 (m, H-3′, 1 H), 4.01–3.98 (m, H-4′, 1 H), 3.76–3.62 (m, H-5′, H-5″ 2 H), 2.72–2.40 (m, H-2′, H-2″, 2 H). Analysis: calculated for $C_8H_{11}N_3O_5$: C, 41.92; H, 4.84; N, 18.33; found: C, 41.71; H, 4.88; N, 18.06.

*1-(2′-Deoxy-5′-dimethoxytrityl-β-D-ribofuranosyl)-4-nitropyrazole (**14**).* 1-(2′-Deoxy-β-D-ribofuranosyl)-4-nitropyrazole (**10**) (0.15 g, 0.86 mmol) was dried by repeated co-evaporation with dry pyridine (3 × 2 ml) and dissolved in anhydrous pyridine (20 ml). 4,4′-Dimethoxytrityl chloride (0.367 g, 1.03 mmol), 4-dimethylaminopyridine (7 mg) and freshly distilled triethylamine (0.25 ml) were added and the solution was stirred under a nitrogen atmosphere. An analysis of the crude reaction mixture by TLC ($CHCl_3$/ethanol 10:1) showed the absence of the free nucleoside and presence of one new component in the mixture after 3 h. The reaction mixture was cooled to 0°C, quenched by the dropwise addition of water (40 ml) and extracted (3 × 40 ml) with ethyl ether. The organic layers were combined, dried over $Na_2SO_4$ and evaporated under reduced pressure to an oily residue. The residue was dissolved in $CH_2Cl_2$ and separated by column chromatography on silica gel (hexanes/acetone). 1-(2′-Deoxy-5′-dimethoxytrityl-β-D-ribofuranosyl)-4-nitropyrazole (**14**) was obtained as a white solid (0.323 g, 71%): $R_f$ = 0.47 ($CHCl_3$/methanol 9:1); MS-FAB *m/z* 303.3 ($DMTr^+$), 531.3 ($M^+$); high resolution MS-FAB *m/z* $M^+$ (calculated 531.2006, found 531.2023); $^1$H NMR 500 MHz (acetone-$d_6$) δ 8.82 (s, H-3, 1 H), 8.22 (s, H-5, 1 H), 7.44-7.21 (m, aromatic DMTr, 9 H), 6.87–6.85 (m, aromatic DMTr, 4 H), 6.15 (triplet, H-1′, *J* = 5.74 Hz, 1 H), 4.63–4.57 (m, H-3′, 1 H), 4.07–4.04 (m, H-4′, 1 H), 3.77 (s, aromatic $OCH_3$, 6 H), 3.21–3.18 (m, H-5′, H-5″, 2 H), 2.78–2.34 (m, H-2′, H-2″, 2 H).

*1-(2′-Deoxy-5′-dimethoxytrityl-β-D-ribofuranosyl-3′-O-2-cyanoethyl-N,N-diisopropylphosphoramidite)-4-nitropyrazole (**18**).* 1-(2′-Deoxy-5′-dimethoxytrityl-β-D-ribofuranosyl)-4-nitropyrazole (**14**) (0.20 g, 0.38 mmol) was dried by repeated co-evaporation with acetonitrile (3 × 2 ml) *in vacuo* and dissolved in anhydrous $CH_2Cl_2$ (2.5 ml). To this solution was added diisopropylammonium tetrazolide (33 mg, 0.19 mmol) along with 2-cyanoethyl *N,N,N′,N′*-tetraisopropylphosphorodiamidite (0.037 g, 0.46 mmol). The solution was allowed to stand under nitrogen at ambient temperature with occasional gentle swirling. After 1.5 h, an analysis of the crude reaction mixture by TLC (acetone/hexane 1:1) showed the complete absence of starting material and the presence of one new component in the mixture. The reaction mixture was cooled to 0°C and quenched by the dropwise addition of methanol/0.5% TEA (1 ml). The solution was evaporated under reduced pressure to an oily residue. The residue was dissolved in $CH_2Cl_2$ (10 ml) and the organic phase washed with a saturated solution of $NaHCO_3$ (2 × 10 ml), dried over $Na_2SO_4$ and evaporated under reduced pressure to an oily residue. The residue was purified by chromatography on a chromatotron plate (2 mm, silica gel) eluting with hexane/ethyl acetate/TEA (1%). Compound **18** was obtained as a yellow solid (0.243 g, 88%): $R_f$ = 0.67 (hexane/acetone, 1:1); MS-FAB *m/z* 303.0 ($DMTr^+$), 732.2 ($MH^+$); high resolution MS-FAB *m/z* $MH^+$ (calculated 732.3162, found 732.3192); $^{31}$P NMR 250 MHz (acetone-$d_6$) δ 150.05, 149.90 (phosphoramidite diastereomers). $^1$H NMR 250 MHz (acetone-$d_6$) δ 8.82–8.79 (m, H-2, 1 H), 8.16–8.13 (m, H-5, 1 H), 7.47–6.82 (m, aromatic DMTr, 13 H), 6.34–6.24 (m, H-1′, 1 H), 4.88–4.81 (m, H-3′, 1 H), 4.29–4.22 (m, H-4′, 1 H), 3.87–3.63 (m, $OCH_2$ and CH, 4 H), 3.74 (m, aromatic $OCH_3$, 6 H), 3.33–3.25 (m, H-5′, H-5″, 2 H), 2.86–2.61 (m, $CH_2CN$ and H-2′ and H-2″, 4 H), 1.28–1.17 (m, $CH_3$, 12 H).

*1-(2′-Deoxy-3,5-di-O-p-toluoyl-β-D-ribofuranosyl)-4-nitroimidazole (**7**).* The procedure described above for the preparation of compound **6** was followed with 4-nitroimidazole to yield 1-(2′-deoxy-3,5-di-*O*-*p*-toluoyl-β-D-ribofuranosyl)-4-nitroimidazole (**7**) as a white solid (0.475 g, 46%). Recrystallization from $CHCl_3$ gave colorless needles: $R_f$ = 0.53 ($CHCl_3$/methanol 20:1); MS-FAB *m/z* 353.0 ($C_{21}H_{21}O_5^+$), 466.0 ($MH^+$); $^1$H NMR 500 MHz ($CDCl_3$) δ 7.96–7.93 (m, p-Tol, 4 H), 7.90 (d, H-5, $J_{5,2}$ = 1.65 Hz, 1 H), 7.88–7.85 (m, p-Tol, 4 H), 7.64 (d, H-2, $J_{2,5}$ = 1.65 Hz, 1 H), 7.31–7.30–7.24 (m, p-Tol, 4 H), 6.15 (triplet, H-1′, *J* = 6.8 Hz, 1 H), 5.72–5.67 (m, H-3′, 1 H), 4.75–4.62 (m, H-4′, H-5′, H-5″, 3 H), 2.85–2.62 (m, H-2′, H-2″, 2 H), 2.44 (s, $CH_3$ p-Tol, 3 H), 2.42 (s, $CH_3$ p-Tol, 3 H). Analysis: calculated for $C_{24}H_{23}N_3O_7$: C, 61.92; H, 4.98; N, 9.03; found: C, 61.80; H, 4.59; N, 9.06.

*1-(2′-Deoxy-β-D-ribofuranosyl)-4-nitroimidazole (**11**).* Compound **11** was obtained in 58% yield as a white solid from compound **7** by the procedure described above for the synthesis of **10**. Recrystallization from ethanol/$H_2O$ gave colorless needles: $R_f$ = 0.23 ($CHCl_3$/methanol 9:1); UV $\lambda_{max}$ $H_2O$ 290 nm; MS-FAB *m/z* 230.0 ($MH^+$); $^1$H NMR 250 MHz ($D_2O$) δ 8.18 (d, H-5, $J_{5,2}$ = 1.54 Hz, 1 H), 7.78 (d, H-2, $J_{2,5}$ = 1.54 Hz, 1 H), 6.05 (triplet, H-1′, *J* = 6.30 Hz, 1 H), 4.38–4.33 (m, H-3′, 1 H), 3.97–3.91 (m, H-4′, 1 H), 3.65–3.49 (m, H-5′, H-5″, 2 H), 2.46–2.20 (m, H-2′, H-2″, 2 H). Analysis: calculated for $C_8H_{11}N_3O_5$: C, 41.92; H, 4.84; N, 18.33; found: C, 42.08; H, 4.91; N, 17.98.

*1-(2′-Deoxy-5′-dimethoxytrityl-β-D-ribofuranosyl)-4-nitroimidazole (**15**).* 1-(2′-Deoxy-β-D-ribofuranosyl)-4-nitroimidazole (**11**) was transformed to the DMTr derivative **15** in 43% yield by the procedure described above for the transformation of **10** to **14**: $R_f$ = 0.45 ($CHCl_3$/methanol 9:1); MS-FAB *m/z* 303.0 ($DMTr^+$), 531.0 ($M^+$); high resolution MS-FAB *m/z* $M^+$ (calculated 531.2006, found 531.2023); $^1$H NMR 250 MHz (acetone-$d_6$) δ 8.24 (d, H-5, $J_{5,2}$ = 1.53 Hz, 1 H), 7.90 (d, H-2, $J_{2,5}$ = 1.53 Hz, 1 H), 7.47–7.21 (m, aromatic DMTr, 9 H), 6.88–6.85 (m, aromatic DMTr, 4 H), 6.26 (triplet, H-1′, *J* = 6.23 Hz, 1 H), 4.65–4.59 (m, H-3′, 1 H), 4.20–4.17 (m, H-4′, 1 H), 3.79 (s, aromatic $OCH_3$, 6 H), 3.34–3.31 (m, H-5′ and H-5″, 2 H), 2.78–2.57 (m, H-2′ and H-2″, 2 H).

*1-(2′-Deoxy-5′-dimethoxytrityl-β-D-ribofuranosyl-3′-O-2-cyanoethyl-N,N-diisopropylphosphoramidite)-4-nitroimidazole (**19**).* Compound **19** was obtained from **15** in 84% yield by the procedure described above for the transformation of **14** to **18**: $R_f$ = 0.58 (hexane/acetone 1:1); MS-FAB *m/z* 303.0 ($DMTr^+$), 732.2 ($MH^+$); high resolution MS-FAB *m/z* $MH^+$ (calculated 732.3162, found 732.3215); $^{31}$P NMR 250 MHz (acetone-$d_6$) δ 150.05, 149.94 (phosphoramidite diastereomers); $^1$H NMR 250 MHz (acetone-$d_6$) δ 8.28–8.26 (m, H-5, 1 H), 7.93–7.91 (m, H-2, 1 H), 7.49–6.85 (m, aromatic DMTr, 13 H), 6.31 (triplet, H-1′, *J* = 6.30 Hz, 1 H), 4.79–4.73 (m, H-3′, 1 H), 4.32–4.22 (m, H-4′, 1 H), 3.78

(s, aromatic $OCH_3$, 6 H), 3.95–3.53 (m, $OCH_2$ and CH, 4 H), 3.40–3.25 (m, H-5′ and H-5″, 2 H), 2.83–2.61 (m, $CH_2CN$ and H-2′ and H-2″, 4 H), 1.36–1.17 (m, $CH_3$, 12 H).

### Synthesis and characterization of oligodeoxyribonucleotides

Oligodeoxyribonucleotides were prepared from commercially available dI, dA, dC, dG and T phosphoramidites (Glen Research) on a Milligen/BioSearch 8700 DNA synthesizer (1 mM scale) by standard solid phase phosphoramidite chemistry (8–10). Coupling yields ranged from 96 to 98%. The detritylated oligonucleotides were detached from the CPG and deprotected by treatment with concentrated $NH_3$ at 55°C for 8 h. The oligonucleotides were purified using 20% polyacrylamide–8 M urea preparative gel electrophoresis. The desired oligonucleotides were extracted from the gels and desalted with Waters C18 SepPaks™ following the manufacturer's instructions. The purified oligomers were evaporated to dryness at 45°C using a Speed Vac™ drying apparatus and stored at –10°C. Oligodeoxyribonucleotides were characterized by MALDI mass spectrometry and/or by HPLC analysis of the constitutent nucleosides obtained by digestion with snake venom phosphodiesterase and bacterial alkaline phosphatase (11). Prior to HPLC analysis, gel purified oligomers (1.0 $A_{260}$ units) were dissolved in 78.2 ml digestion buffer (32 mM Tris, 15 mM $MgCl_2$, pH 7.5). The mixture was incubated at 37°C for at least 8 h (but not exceeding 18 h) with snake venom phosphodiesterase (12 ml) and bacterial alkaline phosphatase (2.0 U) to give a mixture of free nucleosides. Cold 2.5 M sodium acetate, pH 5.0, (10 ml) and 95% ethanol (234 ml) was added, the mixture was allowed to stand at –70°C for 0.5 h and centrifuged at 10 000 *g* for 15 min. The supernatant was decanted off from the insoluble mixture of proteins, diluted to 1 ml by addition of cold 95% ethanol and centrifuged again at 10 000 *g* for 15 min. The supernatant was decanted off and discarded, while the resulting insoluble nucleoside pellet was dried *in vacuo* at 10 000 *g* (35°C), then stored at –10°C or dissolved in 1 ml HPLC grade deionized water and analyzed immediately by HPLC. An analytical Phenomenex C18 column on a Beckman Gold™ HPLC system equipped with a diode array UV scanning device and a dual channel UV detector set to 254 and 234 nm was used for the HPLC analysis. The gradient system consisted of methanol/phosphate buffer ($KH_2PO_4$, pH 7.0) which was ramped from 0 to 30% (v/v) methanol over a 30 min time period. Approximately 20 ml each solubilized digestion product were injected onto the column. The solvent flow rate was 1.0 ml/min. The HPLC system was equipped with a diode array UV scanning device and a dual channel UV detector. One channel of the detector was set to 254 nm, for maximum sensitivity for unmodified nucleosides, while the other channel was adjusted to a value corresponding to the $\lambda_{max}$ of a given modified nucleoside. The components of each digestion product were identified both on the basis of their retention times on the column and by comparison with the UV spectrum of each component (utilizing the on-board UV scanning device) to those of authentic nucleoside standards. The relative composition of each oligomer was inferred by dividing the integrated peak area ($A_{254}$) of each nucleoside component by its extinction coefficient at 254 nm.

### Thermal denaturation studies

*Solution preparation.* The stock solutions were prepared by dissolving each oligonucleotide in pH 7 buffer consisting of 1.0 M NaCl, 10 mM sodium phosphate and 0.1 mM EDTA. The concentration of oligonucleotides was determined by UV spectroscopy, based on an assumption that at high temperature oligonucleotides are unpaired and unstacked. An aliquot of the stock solution (50–70 μl) was diluted to 2.7 ml and the UV melting curve recorded. The upper baseline in each UV melting curve was fitted to a straight line ($y = a + bx$). The absorbance at 25°C was then calculated using this equation. The extinction coefficient of oligonucleotide at 25°C was taken as the sum of the mononucleotides in the strand. Beer's law was applied to calculate the concentration of oligonucleotide for each solution. All stock solutions were refrigerated (4°C) during the course of the experiments.

*UV melting measurements.* Absorbance versus temperature profiles (12,13) were recorded in 1 cm path length fused quartz cuvettes at 260 nm on a Cary 3TM UV-visible spectrophotometer equipped with a Peltier temperature controlling device and thermal software. All the samples were degassed in a vacuum desiccator before use. The oligodeoxyribonucleotide strand concentration was ~15 mM. A layer of silicone oil (Dow 200 fluid, 100 CSTKS) was placed on the surface of the aqueous solution to prevent solvent evaporation. Nitrogen was continuously run through the measurement chamber to prevent condensation of water vapor at low temperature. Prior to the thermal denaturation studies, each sample was heated to 75 or 80°C and allowed to equilibrate at this temperature for at least 10 min. Each sample was then cooled and allowed to equilibrate at the starting temperature for at least 10 min. Absorbance versus temperature curves for the oligomers were obtained with both a heating and cooling ramp rate of 0.5°C/min. Absorbance readings were taken at 1 min intervals. Reversibility of each helix–coil transition was demonstrated since the absorbance values of the melting curves (up ramp) were found to differ from the annealing curves (down ramp) by <2%.

*Data analysis.* The data from the Cary 3 spectrometer were analyzed as previously described (14). $T_m$ values are reported at 15 mM strand concentration and thermodynamic parameters at 298 K, 1 M salt.

## RESULTS AND DISCUSSION

### Synthesis

Preparation of the deoxyribonucleosides of 3-nitropyrrole and 5-nitroindole and their incorporation into oligonucleotides via DMT-protected phosphoramidites have recently been described (1,3). The deoxyribonucleosides of 4-nitropyrazole, 4-nitroimidazole and pyrazole (15) were prepared by the sodium salt glycosylation procedure (16) following the procedure described previously for synthesis of 3-nitropyrrole deoxyribonucleoside (**9**) (1; Fig. 1). The sodium salt glycosylation reaction between 4-nitropyrazole and 1-chloro-2-deoxy-3,5-di-*O*-*p*-toluoyl-α-D-erythropentosyl chloride (**1**) (7) gave a single product in 75% yield. The product was identified as 1-(2′-deoxy-3,5-di-*O*-*p*-toluoyl-β-D-ribofuranosyl)-4-nitropyrazole (**6**) on the basis of the high resolution mass spectrum (*m/z* $MH^+$ 466.1609), elemental analysis and proton NMR spectrum. The anomeric configuration was assigned as β by $^1H$ NMR analysis on the basis of a characteristic triplet for the 1′ proton observed at 6.48 p.p.m. ($J = 6.0$ Hz ) and the narrow multiplet (0.32 p.p.m. width) observed for the two 2′ protons (17,18).

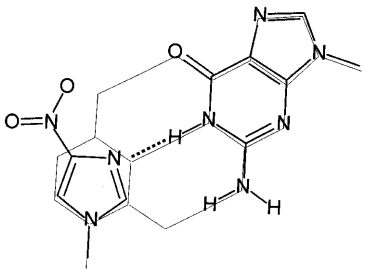

**Figure 2.** Proposed base pairing between 4-nitroimidazole and deoxyguanosine.

Deoxyribosylation and ribosylation reactions involving the mercuric salt of 4(5)-nitroimidazole were previously reported to occur regiospecifically, ultimately leading to formation of 1-(2′-deoxy-β-D-ribofuranosyl)-4-nitroimidazole (**11**) and 1-β-D-ribofuranosyl-4-nitroimidazole (19). However, the sodium salt displacement reaction between 4(5)-nitroimidazole and 1-chloro-2-deoxy-3,5-di-*O*-*p*-toluoyl-α-D-erythropentosyl chloride (**1**) yielded a 2:1 mixture of the 1,4 and 1,5 regioisomers. These were readily separated by column chromatography and recrystallization. The regiochemical assignments of the isomers was based on a comparison of their cross-ring proton–proton coupling constants (20). For the 1,5-disubstituted regioisomer the cross-ring C2 proton–C4 proton coupling constant was calculated to be 0.83 Hz, while the C2–C5 proton coupling constant for the desired regioisomeric 1,4-disubstituted product was found to be 1.65 Hz. According to the empirically based rule, 1,5-disubstituted imidazoles (including *N*-alkyl nitroimidazoles) exhibit cross-ring proton–proton coupling constants significantly <1.0 Hz. Conversely the coupling constants for 1,4-disubstituted regioisomers are typically >1 Hz (20,21).

The anomeric configurations of the two regioisomers were also assigned based on an analysis of their respective $^1$H NMR spectra. The anomeric C-1′ protons of both nucleoside **11** and the 1,5-regioisomer demonstrated characteristically broad triplet NMR signals, with proton–proton coupling constant values of 6.8 and 6.5 Hz respectively. The deoxyribosylation reaction apparently proceeded stereospecifically, since no α anomeric products were isolated from the reaction mixture. Both products were further characterized by MS-FAB and elemental analysis.

For incorporation into oligonucleotide, the nucleoside were converted to 5′-dimethoxytrityl-3′-phosphoramidites as outlined in Figure 1. Modified oligonucleotides were constructed by conventional protocols in an automated DNA synthesizer. Stepwise yields, evaluated by spectrophotometric monitoring of dimethoxytrityl release at each cycle of synthesis, were equivalent to those obtained using phosphoramidites of conventional bases.

## Thermal denaturation studies

UV thermal melting studies were pursued in order to assess the effects of nitroazoles on duplex stability relative to the natural base pairs and base pairs between deoxyinosine and the natural bases. For these studies, a modified version of the Dickerson deoxydodecamer (22) d(CGCXAATTYGCG)$_2$ (X = **9**, **10**, **11**, **12**, **21**, **22**(I), **23**, A, C or G; Y = A, C, G or T) was chosen. The structures of many variants of this sequence, containing either matched or severely mismatched base pairs, have been studied extensively by X-ray crystallography, NMR spectroscopy and optical thermal melting methodology (22–27). These studies have demonstrated that helix–coil transitions involving the Dickerson deoxydodecamer are generally bimolecular in nature and that the duplex exists in a B-form helix. Since each 12mer duplex will contain two modified base pairs, the differences in stability will be magnified by a factor of two, allowing one to more closely discern differences between closely related structures.

From the melting data (Table 1) it is readily apparent that the oligonucleotides containing the modified bases have significantly lower $T_m$ values than the natural sequence. The lower temperature portion of the curves were in many cases insufficiently complete to allow accurate extrapolation for determination of the lower baseline. Consequently, the differential method was used to obtain a $T_{max}$ value, which in turn can be used to calculate $T_m$ as previously described (14).

The thermodynamic values extracted from these curves along with the $T_m$ values are listed in Table 1, along with data for the corresponding sequences containing the natural base pairs A·T and C·G.

The data from this study would appear to implicate 3-nitropyrrole as being unique among nucleoside analogs for its lack of discrimination against each of the four natural bases. The four $T_m$ curves are nearly superimposibile and $\Delta\Delta G$ between the least and most stable is only 0.4 kcal/mol. In comparison, even an A·T base pair differs from a C·G base pair by 1.1 kcal/mol (Table 1). Although not as non-discriminating as 3-nitropyrrole, 5-nitroindole showed relatively small $\Delta G$ differences for pairing with the natural bases. The $\Delta\Delta G$ value between the most and least stable base pair was 0.8 kcal/mol. These $\Delta\Delta G$ differences are so small that, as one might expect, sequence context can alter the apparent order of base stability. For example, in this study, in which the modified base is stacked between cytidine and adenosine, the

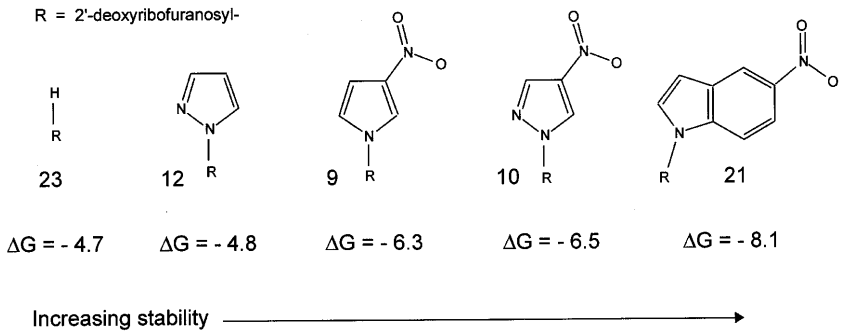


**Figure 3.** Comparison of the average $\Delta G$ values for each set of four oligonucleotides containing each of the modified bases opposite the four natural bases.

base pairing preferences for 3-nitropyrrole were C >T = G > A, whereas, Van Aerschot *et al*. found the order to be A > G > T > C when the modified base was in the context 5′-...GXG...-3′ (5). These differences in base pairing preference for both 3-nitropyrrole and 5-nitroindole are summarized in Table 2. From data reported by Van Aerschot *et al*., $\Delta\Delta G$ values can be obtained for an A·T base pair versus a T**9** (3-nitropyrrole) and T·**21** (5-nitroindole) base pair.

$$\Delta G_{A\cdot T} - \Delta G_{T\cdot \mathbf{9}} = 4.5 \text{ kcal/mol}$$
$$\Delta G_{A\cdot T} - \Delta G_{T\cdot \mathbf{21}} = 3.4 \text{ kcal/mol}$$

These values compare quite closely with the corresponding values obtained in our study, for which $\Delta G_{A\cdot T} - \Delta G_{T\cdot \mathbf{9}} = 4.6$ kcal/mol and $\Delta G_{A\cdot T} - \Delta G_{T\cdot \mathbf{21}} = 3.5$ kcal/mol.

In contrast to 3-nitropyrrole, 4-nitroimidazole showed high selectivity for pairing to G. Models provide a clear explanation of why this occurs. With the nitroimidazole in the *syn* conformation (nitro group projecting into the major groove) the N3 nitrogen could assume a position that is nearly ideal for formation of a hydrogen bond with N1 of the opposing deoxyguanosine (Fig. 2). 4-Nitropyrazole, which, like 3-nitropyrrole, does not have a nitrogen lone electron pair in a position suitable for hydrogen bonding to an opposing base, showed much less dramatic base pairing preferences. However, it was not quite as non-selective as nitropyrrole. The sequence with A opposite 4-nitropyrazole was ~1 kcal/mol ($\Delta G_{25°C} = -7.2$) more stable that the sequences with C, G or T.

In order to fully explore the role of the nitroazole in stabilizing duplex DNA, a non-nitro-substituted heterocycle, pyrazole deoxyribonucleoside **12**, and the abasic site mimic **23** were included in this study. The effect of the abasic site analog 1,2-dideoxyribose on duplex stability has been studied in detail (28). The $T_m$ values of the pyrazole-containing oligonucleotides were as much as 20°C lower than the corresponding sequences containing 4-nitropyrazole deoxyribonucleoside (**11**). Perhaps even more striking was the observation that three of the abasic site-containing sequences have higher $T_m$ values than the corresponding sequences containing the pyrazole nucleoside. The sequences containing pyrazole have consistently low $\Delta H$ and $\Delta S$ values. On the other hand, two of the abasic site-containing sequences, d(CGC-**23**AATTCGCG) and d(CGC**23**AATTAGCG), have relatively large values for both $\Delta H$ and $\Delta S$. Unlike most other melting curves obtained in this study, the curves resulting from these sequences are more complex than one would expect for a two state model. Consequently, the values obtained for $\Delta H$ and $\Delta S$ may not be accurate. In fact, the values of $\Delta S$ are larger than observed for any of the nitroazoles included in this study and instead fall within the range that is typical for nucleosides involved in hydrogen bonding within the duplex structure.

**Table 1.** Melting temperatures ($T_m$) and thermodynamic parameters for helix–coil transitions of the sequence 5′-d(CGC**X**AATT**Y**GCG)-3′ containing nucleoside **9**, **10**, **11**, **12**, **21**, **22** or **23**

| **X·Y** | $T_m$ (°C) | $\pm\Delta H$ (kcal/mol) | $\pm\Delta S$ (cal/K·mol) | $\pm\Delta G_{25°C}$ (kcal/mol) | $\Delta\Delta G$ (kcal/mol) |
|---|---|---|---|---|---|
| A·T | 65.7 | 72.9 | 193.0 | 15.4 | |
| C·G | 70.5 | 74.7 | 195.3 | 16.5 | 1.1 |
| **9**·A | 19.4 | 25.6 | 65.3 | 6.1 | |
| **9**·C | 24.5 | 36.4 | 100.2 | 6.5 | 0.4 |
| **9**·G | 21.1 | 27.1 | 70.1 | 6.2 | |
| **9**·T | 20.7 | 27.0 | 69.8 | 6.2 | |
| **21**·A | 35.0 | 32.0 | 81.7 | 7.7 | |
| **21**·C | 44.5 | 36.0 | 91.1 | 8.3 | 0.8 |
| **21**·G | 40.1 | 28.1 | 67.6 | 8.0 | |
| **21**·T | 46.4 | 27.9 | 65.1 | 8.5 | |
| **23**·A | 7.0 | 45.8 | 140.9 | 3.8 | |
| **23**·C | 6.6 | 41.0 | 124.1 | 4.0 | 1.8 |
| **23**·G | 11.1 | 26.1 | 69.1 | 5.5 | |
| **23**·T | 13.4 | 27.0 | 71.6 | 5.6 | |
| **22**·A | 52.1 | 54.7 | 146.2 | 11.2 | |
| **22**·C | 62.2 | 77.2 | 208.1 | 15.1 | 7.1 |
| **22**·G | 35.4 | 40.8 | 110.1 | 8.0 | |
| **22**·T | 47.1 | 58.9 | 162.0 | 10.6 | |
| **10**·A | 29.0 | 32.8 | 85.9 | 7.2 | |
| **10**·C | 19.3 | 26.8 | 69.3 | 6.1 | 1.1 |
| **10**·G | 18.5 | 26.6 | 68.4 | 6.2 | |
| **10**·T | 21.4 | 26.7 | 68.0 | 6.4 | |
| **11**·A | 19.5 | 28.3 | 73.9 | 6.3 | |
| **11**·C | 21.1 | 31.1 | 83.3 | 6.3 | 3.0 |
| **11**·G | 40.9 | 49.8 | 135.9 | 9.3 | |
| **11**·T | 17.9 | 28.8 | 76.4 | 6.0 | |
| **12**·A | 8.5 | 27.5 | 75.7 | 5.0 | |
| **12**·C | < 0 | 28.1 | 79.2 | 4.5 | 0.6 |
| **12**·G | 7.2 | 23.1 | 60.2 | 5.1 | |
| **12**·T | 7.7 | 30.5 | 86.6 | 4.7 | |

Absorbance versus temperature profiles of the sequences were determined at 260 nm. Measurements were made in 1 M NaCl, 10 mM $Na_2HPO_4^{-2}$, 1 mM EDTA, pH 7.0, at an oligonucleotide concentration of ~15 μM.

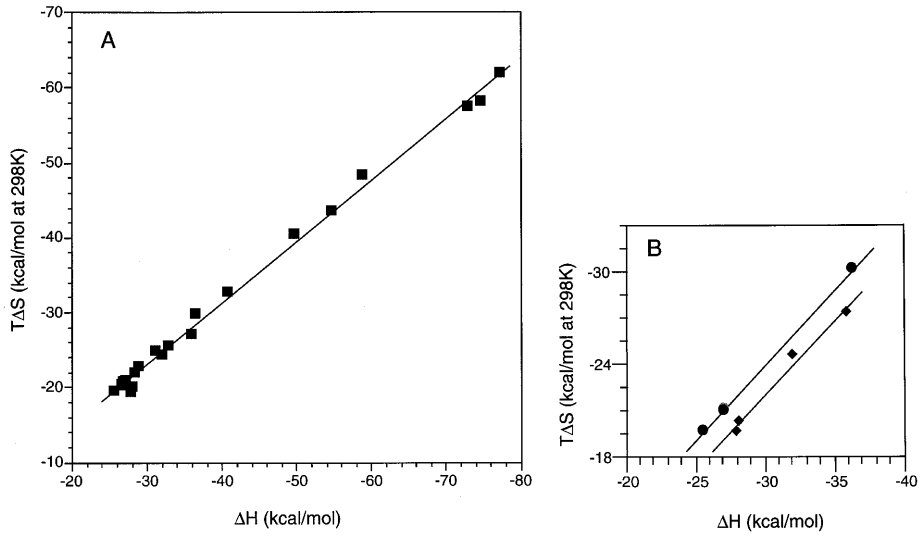


**Figure 4.** (**A**) Plot of Δ*H* versus *T*Δ*S* for the oligonucleotide sequences d(CGC**X**AATT**Y**GCG)$_2$, where Y = A, C, G or T and X = **9**, **10**, **11**, **21**, **22**, A and C. (**B**) Higher resolution plot of Δ*H* versus *T*Δ*S* for the oligonucleotide sequences d(CGC**X**AATT**Y**GCG)$_2$, where Y = A, C, G or T and X = **9** (3-nitropyrrole) and **21** (5-nitroindole).

A comparison of the various nucleoside analogs included in this study is summarized in Figure 3. The average Δ*G* values for each set of four oligonucleotides containing each of the modified bases opposite the four natural bases are listed under the structure of the bases in Figure 3. Since $\Delta G_{25^\circ C}$ for the sequences containing only natural bases fall in the range –15.4 to –16.5 kcal/mol, it is clear that even the most avid binding analog, 5-nitroindole, is a poor substitute for a natural base.

One observation about the thermodynamic parameters that is noteworthy is the correlation between Δ*H* and Δ*S*. Large negative enthalpy values are associated with large negative entropy changes, while small negative enthalpy changes are associated with small negative entropy changes. The most striking aspect of this result is that when one plots Δ*H* versus Δ*S* for all the nitroazole-containing sequences, as well as the sequences containing only natural bases or dI, one obtains a straight line relating *T*Δ*S* to Δ*H* (Fig. 4A). This implies that the correlation between Δ*S* and Δ*H* is independent of the mode of association of the bases. Both the bases that associate by hydrogen bonding as well as those that associate only through base stacking appear to fall on the curve shown in Figure 4. Searle and Williams have rationalized enthalpy–entropy compensation for oligonucleotide duplex formation as stemming from coupling between loss of translational and rotational freedom of the ribose–phosphate backbone and exothermicity of base stacking (29). Our data suggests that hydrogen bonding plays a significant role in the exothermicity of base association. Recent experiments reported by Kool and co-workers show that 4-methylindole stacks as least as effectively as adenosine (30). Hence, the large differences in enthalpy observed for the natural bases versus 5-nitroindole more likely reflect alterations in hydrogen bonding interactions. It is possible that the differences that we observe reflect loss of hydrogen bonding interactions for the base opposite that nitroazole. If a natural base remains stacked in the helix without an opposing hydrogen bonding partner then it has lost hydrogen bonding interactions with water without regaining a new donor/acceptor partner. The relatively low values for Δ*S* (Δ*S* averages 76 cal/K·mol for both 3-nitropyrrole and 5-nitroindole) reflect the greater freedom of movement possible for bases that are not locked into the duplex by hydrogen bonding interactions.

**Table 2.**

| Sequence | Base pairing preferences | |
|---|---|---|
| | 3-Nitropyrrole | 5-Nitroindole |
| CXA | C > T = G > A | T > C > G > A |
| TXT | A > C = T > G | |
| GXG | A > G > C > T | C > A > T = G |
| GXC | A > G > T > C | A > T = G = C |

A detailed comparison of the differences in the values of Δ*H* and Δ*S* for 3-nitropyrrole versus 5-nitroindole is instructive. The values of Δ*H* average 2 kcal/mol higher (1 kcal/mol/bp) for the sequences containing 5-nitroindole in comparison with the sequences containing 3-nitropyrrole. This is consistent with the enhanced stacking interaction expected for the larger aromatic ring of indole. But what is most interesting is that a closer look at the plots of Δ*H* versus *T*Δ*S* for the oligonucleotides containing these two nucleotide analogs reveal that the points for each fall on two parallel line with intercepts on the *x*-axis (Δ*H*) that are separated by 2 kcal/mol (Fig. 4B). It is possible on the basis of our results to speculate on the potential for developing non-hydrogen bonding base analogs with higher binding affinity than 5-nitroindole. Recent studies by Kool and co-workers provide important guidance in this regard. They have shown that pyrene, phenanthrene and naphthalene are all more efficient than the natural bases thymine and adenine when placed at the ends of a helix (30). On comparing the ability of 5′-end dangling bases to stabilize a DNA duplex, Kool *et al.* found ΔΔ*G* (difference in Δ*G* between a sequence containing no dangling base and one that does) to be 3.1 kcal/mol for 4-methylindole, 2.9 kcal/mol for naphthalene, 2.6 kcal/mol for phenanthralene, 3.4 kcal/mol for pyrene and 2.0 kcal/mol for adenine. This results suggests that even with more extensive conjugated aromatic systems one may not expect to gain a great deal more in stability beyond that which indole is able to provide.

## CONCLUSION

Comparison of $T_m$ and thermodynamic data indicate that 3-nitropyrrole and 5-nitroindole are exceptionally non-discriminating base pairing partners. Neither base appears to participate in hydrogen bonding, but on the basis of modeling both should fit into the helix opposite each of the natural bases without distorting the helix. The nitro group plays an important role in stabilization, but in the absence of direct comparison with other substituents it is not yet established if other functional groups would not serve a similar function. Addition of a ring nitrogen that is capable of functioning as a hydrogen bond acceptor decreases the non-discriminating character of the nitroazole base. Nitroimidazole shows highly specific base pairing to G, while 4-nitropyrazole shows some preference for pairing to A. On the basis of these studies it appears that other non-discriminating, non-hydrogen bonding analogs may be possible. However, we believe that there is an inherent limitation to the extent to which non-hydrogen bonding heterocycles which occupy the position of a single natural base can stabilize a helix. At least two other possible alternatives for obtaining non-discriminating nucleoside analogs which bind with higher free energy than the analogs studied here can be envisioned. The first alternative is suggested by the significant contribution of entropy loss to the low free energy gain on duplex formation. The phosphodiester–ribose backbone could be redesigned to fix one or more of the six internal rotations that contribute to the loss of entropy. The second alternative is to build base analogs that allow non-discriminate hydrogen bonding to each of the four natural bases (31,32). This alternative is under investigation and will be the topic of future publications.

## ACKNOWLEDGEMENTS

The National Institutes of Health are gratefully acknowledged for support for this research. Helpful discussions with V.J.Davisson, G.Hoops and N.Paul were also appreciated.

## REFERENCES

1 Bergstrom,D.E., Zhang,P., Toma,P.H., Andrews,C.A. and Nichols,R. (1995*) J. Am. Chem. Soc.*, **117**, 1201–1209.
2 Nichols,R., Andrews,P.C., Zhang,P. and Bergstrom,D.E. (1994) *Nature*, **369**, 492–493.
3 Loakes,D. and Brown,D.M. (1994) *Nucleic Acids Res.*, **22**, 4039–4043.
4 Loakes,D., Brown,D.M., Linde,S. and Hill,F. (1995) *Nucleic Acids Res.*, **23**, 2361–2366.
5 Van Aerschot,A., Hendrix,C., Schepers,G., Pillet,N. and Herdewijin,P. (1995) *Nucleosides Nucleotides*, **14**, 1053–1056.
6 Huttle,R. and Buchele,F. (1955) *Chem. Berl.*, **88**, 1586–1590.
7 Bhat,C.C. (1968) In Zorbach,W.W. and Tipson,R.S. (eds), *Synthetic Proceedures in Nucleic Acid Chemistry.* Interscience Publishers, New York, NY, Vol. 1, pp. 521–522.
8 Gait,M.L. (1984) In Rickwood,D. and Hames,B.D. (eds), *Oligonucleotide Synthesis: A Practical Approach.* IRL Press, Washington, DC.
9 Aul,R. (1993) In Keller,G.H. and Manak,M.M. (eds), *DNA Probes*, 2nd Edn. Stockton Press, New York, NY, pp. 69–136.
10 Brown,T. and Brown,D.J.S. (1991) In Eckstein,F. (ed.), *Oligonucleotides and Analogues.* IRL Press, New York, NY, pp. 1–24.
11 Eadie,J.S., McBride,L.J., Efcavitch,J.W., Hoff,L.B. and Cathcart,R. (1987) *Anal. Biochem.*, **165**, 442–447.
12 Millican,T.A., Mock,G.A., Chauncey,M.A., Patel,T.P., Eaton,M.A.W., Gunning,J., Cutbush,S.D., Neidle,S. and Mann,J. (1984) *Nucleic Acids Res.*, **12**, 7435–7453.
13 Martin,F.H., Uhlenbeck,O.C. and Doty,P. (1971) *J. Mol. Biol.*, **57**, 201–215.
14 Johnson,T.W., Zhang,P. and Bergstrom,D.E. (1997) *Nucleic Acids Res.*, **25**, 559–567.
15 Durland,R.H., Rao,T.S., Bodepudi,V., Seth,D.M., Jayaraman,K. and Revankar,G.R. (1995) *Nucleic Acids Res.*, **23**, 647–653.
16 Ramasamy,K., Robins,R.K. and Revankar,G.R. (1986) *Tetrahedron*, **42**, 5869–5878.
17 Srivastava,P.C. and Robins,R.K. (1981) *J. Heterocyclic Chem.*, **18**, 1659–1662.
18 Robins,M.J. and Robins,R.K. (1965) *J. Am. Chem. Soc.*, **87**, 4934–4940.
19 Guglielmi,H. and Vergin,H. (1972) *Liebigs. Annln Chem.*, **761**, 67–76.
20 Matthews,H.R. and Rapoport,H. (1973) *J. Am. Chem. Soc.*, **95**, 2297–2303.
21 Columbo,R., Columbo,F., Derome,A.E., Jones,J.H., Rathbone,D.L. and Thomas,D.W. (1985) *J. Chem. Soc. Perkin Trans. I*, 1811–1815.
22 Drew,H.R., Wing,R.M., Takano,T., Broka,C., Tanaka,S., Itakura,K. and Dickerson,R.E. (1981) *Proc. Natl. Acad. Sci. USA*, **78**, 2179–2183.
23 Brown,T., Leonard,G.A., Booth,E.D. and Chambers,J. (1989) *J. Mol. Biol.*, **207**, 455–457.
24 Leonard,G.A., Booth,E.D. and Brown,T. (1990) *Nucleic Acids Res.*, **18**, 5617–5623.
25 Hare,D.R., Wemmer,D.E., Chou,S.-M., Drobny,G. and Reid,B.R. (1983) *J. Mol. Biol.*, **171**, 319–336.
26 Brown,T., Leonard,G.A., Booth,E.D. and Kneale,G. (1990) *J. Mol. Biol.*, **212**, 437–440.
27 Patel,D.J., Kozlowski,S.A., Marky,L.A., Rice,J.A., Broka,C., Dallas,J., Itakura,K. and Breslauer,K.J. (1982) *Biochemistry*, **21**, 437–444.
28 Vesnaver,G., Chang,C.-N., Eisenberg,M., Grollman,A.P. and Breslauer,K.J. (1989) *Proc. Natl. Acad. Sci. USA*, **86**, 3614–3618.
29 Searle,M.S. and Williams,D.H. (1993) *Nucleic Acids Res.*, **21**, 2051–2056.
30 Guckian,K.M., Schweitzer,B.A., Ren,R.X.-F., Sheils,C.J., Paris,P.L., Tahmassebi,D.C. and Kool,E.T. (1996) *J. Am. Chem. Soc.*, **118**, 8182–8183.
31 Bergstrom,D.E., Zhang,P. and Zhou,J. (1994) *J. Chem. Soc. Perkin Trans. I*, 3029–3034.
32 Bergstrom,D.E., Zhang,P. and Johnson,W.T. (1996) *Nucleosides Nucleotides*, **15**, 59–68.